TISSUE ENGINEERING
Volume 11, Number 1/2, 2005

Diffusion Limits of an *in Vitro* Thick Prevascularized Tissue

CRAIG K. GRIFFITH, M.S.,[1] CHERYL MILLER, Ph.D.,[2] RICHARD C.A. SAINSON, Ph.D.,[3] JAY W. CALVERT, M.D.,[4] NOO LI JEON, Ph.D.,[1] CHRISTOPHER C.W. HUGHES, Ph.D.,[3] and STEVEN C. GEORGE, M.D., Ph.D.[1]

ABSTRACT

Although tissue engineering promises to replace or restore lost function to nearly every tissue in the body, successful applications are currently limited to tissue less than 2 mm in thickness. *In vivo* capillary networks deliver oxygen and nutrients to thicker (>2 mm) tissues, suggesting that introduction of a preformed *in vitro* vascular network may be a useful strategy for engineered tissues. This article describes a system for generating capillary-like networks within a thick fibrin matrix. Human umbilical vein endothelial cells, growing on the surface of microcarrier beads, were embedded in fibrin gels a known distance (Δ = 1.8–4.5 mm) from a monolayer of human dermal fibroblasts. The distance of the growth medium, which contained vascular endothelial growth factor and basic fibroblast growth factor, from the beads, *C*, was varied from 2.7 to 7.2 mm. Capillaries with visible lumens sprouted in 2–3 days, reaching lengths that exceeded 500 μm within 6–8 days. On day 7, capillary network formation was largely independent of *C;* however, a strong inverse correlation with Δ was observed, with the maximum network formation at Δ = 1.8 mm. Surprisingly, the thickness of the gel was not a limiting factor for oxygen diffusion as these tissue constructs retained a relatively high oxygen tension of >125 mmHg. We conclude that diffusion of oxygen *in vitro* is not limiting, allowing the development of tissue constructs on the order of centimeters in thickness. In addition, diffusion of fibroblast-derived soluble mediators is necessary for stable capillary formation, but is significantly impeded relative to that of nutrients present in the medium.

INTRODUCTION

Continued advances in tissue engineering will lead to new therapies that restore, maintain, or enhance function in damaged tissues. However, the most successful applications have been in thin (<2 mm) tissues, in which delivery of essential nutrients occurs by diffusion. Avascular examples include the epidermis of skin and cartilage found in the nasal septae.[1–3] Tissue engineering of more complex tissues such as cardiac muscle[4–6] and liver has been attempted but has also been limited to thin sections. Treatment of more homogeneous tissues such as adipose tissue[7] and smooth muscle[8] has met with some success but has also been limited to dimensions less than 2 mm. Larger (>1 cm), more complex (structurally and functionally) tissues such as those found in the body cannot be supported by simple diffusion and will require vascular networks to support cellular function. Currently, developing strategies to construct viable tissue-engineered constructs beyond the diffusion limit is perhaps the greatest challenge facing the field of tissue engineering.[9]

[1]Department of Biomedical Engineering, University of California, Irvine, Irvine, California.
[2]Department of Biomedical Engineering, Duke University, Durham, North Carolina.
[3]Department of Molecular Biology and Biochemistry, University of California, Irvine, Irvine, California.
[4]Aesthetic and Plastic Surgery Institute, UCI Manchester Pavilion, Orange, California.

Clinically, the demand for engineered soft tissues with controlled dimensions is enormous. More than 1 million reconstruction and cosmetic surgeries are performed in the United States annually.[10] The majority of these procedures use autologous donor sites as a source of soft tissue for a space-filling application. The donor site creates a secondary wound that increases surgery and recovery times, and increases the risk of infection and potential loss of function. In addition, tissue from donor sites is often avascular and not sterile. Typical procedures that result in soft tissue loss include tumor removal, full and partial mastectomy, and laceration repair. An artificial soft tissue with a preformed vasculature would potentially eliminate the need for autologous tissue transplant.

Currently, there are three approaches for engineering vascularized tissues: (1) stimulating rapid vessel growth in avascular implants with angiogenic factors,[11–17] (2) seeding biodegradable polymer scaffolds, which provide bulk, with endothelial cells and angiogenic factors,[18,19] and (3) prevascularizing the artificial tissue before implantation.[20–22] All of these methods have shown some promising results, but only the latter approach precludes the need for new vessel ingrowth from the host, which limits the survival time of cells in the center of the graft.

Schechner *et al*.[22] demonstrated that human endothelial cords grown *in vitro* in a collagen matrix (<24 h old and 2 mm thick) will incorporate with a host (immune-compromised mouse) on implantation. However, thicker tissues will require fully preformed capillaries with lumens, which do not occur in a collagen matrix. The objective of the present study was 3-fold: (1) develop an *in vitro* system composed of fully formed stable capillaries within a biocompatible matrix (fibrin), (2) demonstrate that diffusion of oxygen *in vitro* is not limiting, and (3) determine the *in vitro* diffusion limits for fibroblast- and medium-derived nutrients for maximal capillary network formation.

MATERIALS AND METHODS

Cell culture

Human dermal fibroblasts (DF, CL#110, American Type Culture Collection [ATCC], Manassas, VA) were cultured in fibroblast growth medium (FGM-2; Cambrex Bio Science Walkersville, Walkersville, MD). Medium was changed three times per week and the cells were harvested with trypsin–EDTA (Cambrex Bio Science Walkersville). Human umbilical cord vein endothelial cells (HUVECs) were isolated from freshly harvested umbilical cords. Collagenase type IA (Sigma, St. Louis, MO) digestion (1 mg/mL) was performed at 37°C for 10 min to release endothelial cells from the vessel walls. Vessel walls were rinsed with Hanks' balanced salt solution (HBSS; Cambrex Bio Science Walkersville) and the wash was collected. The wash was centrifuged at 1200 rpm for 5 min. The pellet was resuspended in endothelial growth medium (EGM-2; Cambrex Bio Science Walkersville) without vascular endothelial cell growth factor (VEGF) and plated in collagen-treated culture flasks (Fisher Scientific, Pittsburgh, PA). On reaching 80% confluency, HUVECs were harvested by trypsin–EDTA treatment. DFs were used up to passage 25, whereas HUVECs were passaged a maximum of three times.

Vascularized tissue construct assembly

Cytodex 3 microcarrier beads (Amersham Biosciences) were sterilized and prepared for seeding with a series of washes in microvascular endothelial cell medium 2 (EGM-2 MV; Cambrex Bio Science Walkersville) modified without VEGF. HUVECs (passage 3) were added (seeding density, 4×10^6) to an inverted 25-cm^2 culture flask containing 5 mL of EGM-2 MV without VEGF and approximately 10,000 Cytodex beads. The inverted flask was then incubated at 37°C in a 5% CO_2 atmosphere. To facilitate bead coating, the flask was shaken gently every 30 min. After 4 h, the microcarrier beads were adequately coated with HUVECs. The coated beads were transferred to a fresh 25-cm^2 flask and incubated in the standard cell culture position for 24 h, allowing any suspended cells to attach to the bottom of the flask. A fibrin solution (2.5 mg of fibrinogen [Sigma] per milliliter of EGM-2 modified without fetal bovine serum) was prepared and sterile filtered. To assemble the construct, the endothelial cell-coated beads (100–200 beads per 0.5 mL of fibrin solution) and 5% FBS were added to the fibrin solution. In each well of a 24-well plate (Fisher Scientific), 10 μL of a thrombin solution (50 U/mL) and the desired volume (milliliters) of the fibrin–bead solution were added. The construct was allowed to stand for 5 min, while the beads settled to the bottom of the well by gravity, before incubation for 20 min at 37°C in 5% CO_2. During incubation the fibrin cross-links ("gels"). The beads were seeded at a relatively low density to maximize the distance between neighboring beads and to minimize clumping.

Fibroblasts were then plated (20,000 cells per well) on top of the fibrin gel in a monolayer a fixed distance (on the order of millimeters) away from the bottom of the well, and thus from the cell-coated beads. The distance of separation was controlled by the volume of fibrin solution added. Fibroblasts were allowed to attach for 3 h and then an acellular layer of fibrin solution of known volume (and thus thickness) was layered above the fibroblasts, completing the tissue construct. Figure 1 demonstrates the completed tissue construct and dimensions schematically. The constructs were maintained with EGM-2 supplemented with aprotinin (0.15 U/mL) to pre-

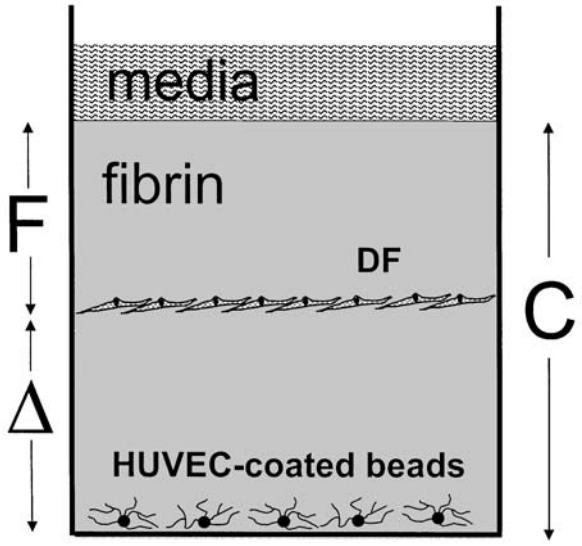

FIG. 1. *In vitro* fibrin gel model. This schematic shows the location of HUVEC-coated beads and the dermal fibroblast monolayer (DF) relative to each other and the nutrient medium. The system is characterized by three physical dimensions: *C*, the distance at which the endothelial cell-coated beads are kept from the growth medium; **F**, the distance separating the fibroblast monolayer from the growth medium; and Δ, the distance between the capillary network and the fibroblast monolayer. The current study examined the impact of *C* and Δ on the quality of the capillary network.

vent the rapid degradation of the gel by endothelial cell-derived proteases.

Diffusion limits

The diffusion distances examined (see Fig. 1) were the distance from the endothelial cell-coated beads to the growth medium, *C*, and the distance between the endothelial cells and the fibroblasts, Δ. If *C* was increased while holding Δ constant, then the distance between the fibroblasts and the growth medium, *F*, also increased and thus *F* was not independently examined. Values of *C* varied from 3.6 to 7.2 mm in 0.9-mm increments. Therefore there were five values of *C* (3.6, 4.5, 5.4, 6.3, and 7.2 mm). For a given *C*, Δ was varied by moving the position of the fibroblast monolayer such that Δ varied between 1.8 and 4.5 mm (0.9-mm increments and thus four distances). Preliminary experiments proved that Δ greater than 4.5 mm produced little capillary formation (data not shown). For each condition, two gels containing 100–200 EC-coated beads were constructed. The result is 1 experiment with 17 conditions (34 gels).

Images and processing

Tissue constructs were imaged 7 days postassembly by phase-contrast microscopy. Of the 100–200 beads per experimental condition, 5 beads were imaged at low power (×10) and saved as high-resolution files (*.tif). To identify the impact of Δ and *C* on the capillary network, each gel was scanned by moving the field of view from top left to bottom right in 1-mm increments. The first five isolated beads (i.e., not exhibiting anastomoses with a neighboring bead) were selected for imaging and quantification. Image-processing software (Scion Image; Scion, Frederick, MD) was utilized to quantify the capillary/bead images. A total of 85 beads (17 combinations of *C* and Δ [see Fig. 5], times 5 beads per condition) were quantified using three indices (Fig. 2): (1) total capillary network length (sum of all vessel segments), (2) total number of vessel segments per bead, and (3) number of vessel sprouts (vessels >100 μm in length whose origin could be traced to the bead) per bead. These parameters were measured directly from the high-resolution image files by four different research personnel following the same protocol, and the values were averaged. Personnel quantifying the vessels were "blinded" as to the experimental conditions.

Oxygen tension

To determine whether oxygen was diffusion limited in this model, acellular fibrin gels with a total depth of 9 mm, and standard (i.e., with HUVEC-coated beads and DFs) gels where $C = 9$ mm, and $\Delta = 1.8$ or 5.4 mm, were generated. Oxygen tension was measured with a fiber optic oxygen sensor (FOXY; Ocean Optics, Dunedin, FL). The tissue constructs were maintained for 2 days, and then the oxygen sensor was inserted just below the surface of the tissue and allowed to reach a steady state reading. The oxygen probe was then progressively lowered into the tissue at precise depths and steady state oxygen tensions were recorded. This process was re-

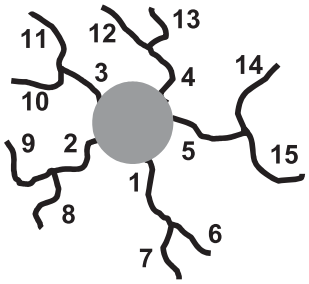

FIG. 2. Technique to quantify capillary network. A schematic showing capillaries radiating from a single bead at ×10 (low power). Beads from each construct are quantified by three characteristics: (1) the number of sprouts that can be traced back to the bead, (2) the number of individual vessel segments, and (3) the total length of all the vessel segments. The numbers (1–15) indicate individual segments, and vessels 1–5 indicate a sprout.

peated at three different radial positions. The result is data demonstrating oxygen tension as a function of depth into the gel.

Statistics

To determine whether features of the capillary network depended on Δ or C, data were plotted holding either C constant and varying Δ, or holding Δ constant and varying C. Linear regression on the aggregate data was then performed and confidence intervals for the slope were determined. A 95% confidence interval that did not include zero was deemed statistically significant.

RESULTS

HUVECs seeded on microcarrier beads rapidly sprout and form capillary networks in fibrin-based tissue constructs. Sprouts form within 2–3 days postassembly. After 6–8 days fully formed capillaries, lined with multiple endothelial cells consistent with patent lumens, reach lengths of up to 500 μm (Fig. 3A–C). When left in culture for up to 14 days, the capillary network continues to remodel, developing an extensive anastomosing network among neighboring beads (Fig. 3D). Endothelial cells in gels made without fibroblasts migrated off the beads, and failed to align and organize into stable capillaries (Fig. 3E).

To investigate the impact of thickness on diffusion of nutrients and growth factors from the medium and the DF, we systematically varied the distance separating the beads from the medium, C, and the monolayer of DF, Δ. Images showing representative beads for selected values of C (Δ held constant) and Δ (C held constant) are shown in Fig. 4. It is evident that robust capillary network development occurs for $\Delta = 1.8$ at several values of C; however, as Δ increases, the extent of the capillary network is compromised, again independent of C.

Figure 5 quantifies the impact of either C (Fig. 5A, C, and E, where each line represents a different constant value of Δ) or Δ (Fig. 5B, D, and F, where each line represents a different constant value of C) on the three features of the capillary network described in Materials and Methods (1) total capillary network length (Fig. 5A and B), (2) total number of vessel segments per bead (Fig. 5C and D), and (3) number of vessel sprouts per bead (Fig. 5E and F). It is evident that all three features of the capillary network behave similarly; that is, there is a strong correlation between total network length, number of vessel segments, and number of sprouts. The other striking result is the marked dependence (statistically significant for all features of the network) of the capillary network on Δ, as previously described qualitatively in Fig. 4. When the distance between the beads and the DF monolayer exceeds 1.8 mm, the extent of the capillary network is compromised. This is evident in Fig. 5B, D, and F, which demonstrates a steady decrease in the capillary network parameters (e.g., total network length) for $\Delta > 1.8$ mm. The capillary network is independent (statistically insignificant) of the thickness, C, for values between 3.6 and 7.2 mm.

One potential limiting nutrient is oxygen, which could be consumed by the DF monolayer that separates the HUVEC-coated beads from the source of oxygen. Hence, we measured the oxygen tension as a function of depth in the gel in the presence and absence of cells. As shown in Fig. 6, the oxygen tension remains $>$125 mmHg (room oxygen tension is approximately 160 mmHg) throughout the fibrin-based tissue construct in the absence or presence of cells. This suggests that the diffusion limitation observed in Fig. 5 is due to nutrients (e.g., growth factors) derived primarily from the fibroblasts, not oxygen. To determine *in vivo* diffusion limits, one must be able to create larger viable tissues *in vitro*. Hence, this result demonstrates the feasibility of this premise, as the implanted tissue construct will encounter partial pressures of oxygen *in vivo* ($\sim$25 mmHg) that are much lower than we have demonstrated *in vitro*.

DISCUSSION

Overcoming diffusion limits for the delivery of essential nutrients and the removal of waste products is a primary obstacle in the development of thick ($>$2 mm) engineered tissues. One possible solution is to mimic the strategy used successfully *in vivo*: namely, convection of nutrients and waste products in a vascular network. The present study addresses this issue with the development of an *in vitro* three-dimensional model of angiogenesis that could form the foundation of a strategy to prevascularize a tissue construct before implantation. The model is composed of HUVEC-coated microcarrier beads and a fibroblast monolayer embedded in a fibrin matrix. Capillary sprouts are observed within 2–3 days of culture and, when left in culture for 6 days, the sprouts continue to develop into fully formed capillaries with observable lumens. This initial study investigated *in vitro* diffusion limits of the developing capillary network to determine the impact of two critical distances in the model system: (1) the distance separating the fibroblasts from the capillary network (Δ), and (2) the distance separating the nutrient medium from the capillary network (C). We found that three characteristics of the capillary network (total length of capillary network, number of capillary sprouts, and average length of capillaries) were significantly reduced for $\Delta = 1.8$ mm, but were independent of C up to 7.2 mm.

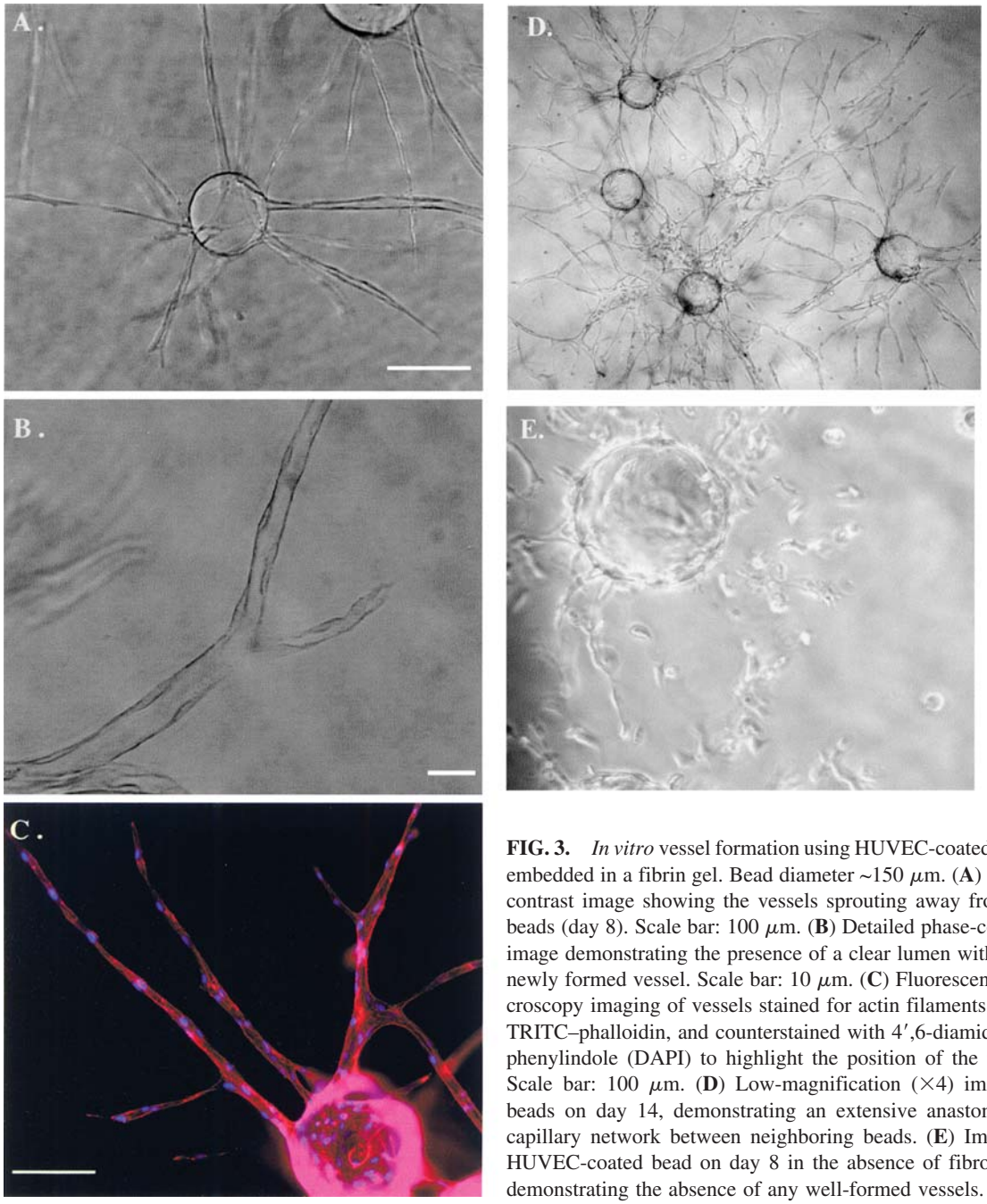

FIG. 3. *In vitro* vessel formation using HUVEC-coated beads embedded in a fibrin gel. Bead diameter ~150 μm. (**A**) Phase-contrast image showing the vessels sprouting away from the beads (day 8). Scale bar: 100 μm. (**B**) Detailed phase-contrast image demonstrating the presence of a clear lumen within the newly formed vessel. Scale bar: 10 μm. (**C**) Fluorescence microscopy imaging of vessels stained for actin filaments, using TRITC–phalloidin, and counterstained with 4′,6-diamidino-2-phenylindole (DAPI) to highlight the position of the nuclei. Scale bar: 100 μm. (**D**) Low-magnification (×4) image of beads on day 14, demonstrating an extensive anastomosing capillary network between neighboring beads. (**E**) Image of HUVEC-coated bead on day 8 in the absence of fibroblasts, demonstrating the absence of any well-formed vessels.

In vitro *prevascularization*

Our *in vitro* model of angiogenesis utilizes materials (i.e., fibrin, HUVECs, and DFs) that mimic the normal wound-healing angiogenic response *in vivo*, and thus offers several advantages. Fibrin is the primary component of the provisional matrix that is initially present in a healing wound. In addition to the primary anticoagulant function, fibrin also stimulates the in growth of new vessels to vascularize the wound area.

Cytodex beads are made of dextran and are completely biocompatible. Although new vessels in the *in vitro* model can be traced back to (or dead end) at a bead, time-lapse microscopy of the network (data not shown) demonstrates continuous dynamic formation and dissolution of anastomoses between neighboring beads. This observation suggests that once implanted *in vivo*, remodeling of anastomoses by the host will allow the network to rapidly circumvent the Cytodex beads. It is also of interest to note that directly embedding endothelial cells in

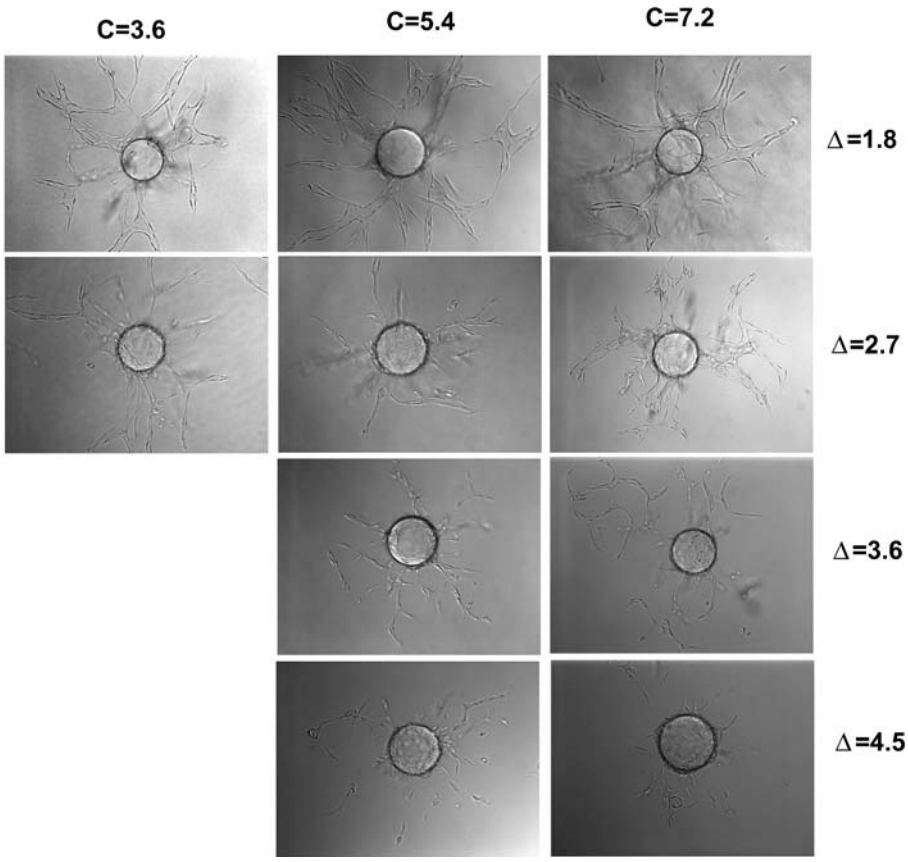

FIG. 4. Images of vascular network with increasing diffusion distances. Images show representative beads that were quantified on day 7 and used to generate Fig. 5. The fibrin matrix depth, *C*, increases from 3.6 to 7.2 mm horizontally, while Δ increases from 1.8 to 4.5 mm vertically. From these images it is apparent that diffusion limits exist for mediators produced by the fibroblast monolayer as the quality of the vessel network is compromised as Δ exceeds 1.8 mm, but do not exist for mediators present in the medium as the vessel network remains robust and independent of *C*.

fibrin gels (i.e., without coating on Cytodex beads) does not yield a similar capillary network. This likely reflects the need for the endothelial cell to go through the full program of sprouting, migration, alignment, and tube formation, rather than being forced to "coalesce" into a vessel from an initial random distribution of cells in the gel.

HUVECs were chosen because they are easily maintained, can be cultured in large numbers, and are obtained from discarded tissue. Clearly, the fact that autologous donation, in the absence of long-term cryopreservation, is not possible represents a significant disadvantage. However, our primary goal is to establish the feasibility of prevascularizing a tissue construct. Advances in the collection, identification, and proliferation of circulating endothelial precursor cells (EPCs) is encouraging,[23–25] and the applicability of EPCs for prevascularizing a tissue construct remains an attractive and viable option.

Competing technologies to overcome diffusion barriers

Numerous methods have been proposed to use vascularization as a strategy to overcome the diffusion barrier

FIG. 5. A diffusion limit exists for nutrients and mediators from the medium and fibroblasts to the capillary network. Day 7 values for total vessel length (**A** and **B**), total number of vessel segments (**C** and **D**), and total number of sprouts (**E** and **F**) of the capillary network are shown as a function of the distance separating the capillary network from the nutrient medium, *C* (**A**–**C**), and the distance separating the fibroblasts from the capillary network, Δ (**D**–**F**). In (**A**–**C**) the lines represent different values of Δ, and in (**D**–**F**) the lines represent different values of *C*. In this fashion, one can visualize the dependence of the capillary network on both Δ and *C* while holding the other variable constant. The quality of the capillary network is compromised (statistically significant negative slope using linear regression on the aggregate data) as Δ becomes larger than 1.8 mm, but is independent of *C* for distances as large as 7.2 mm.

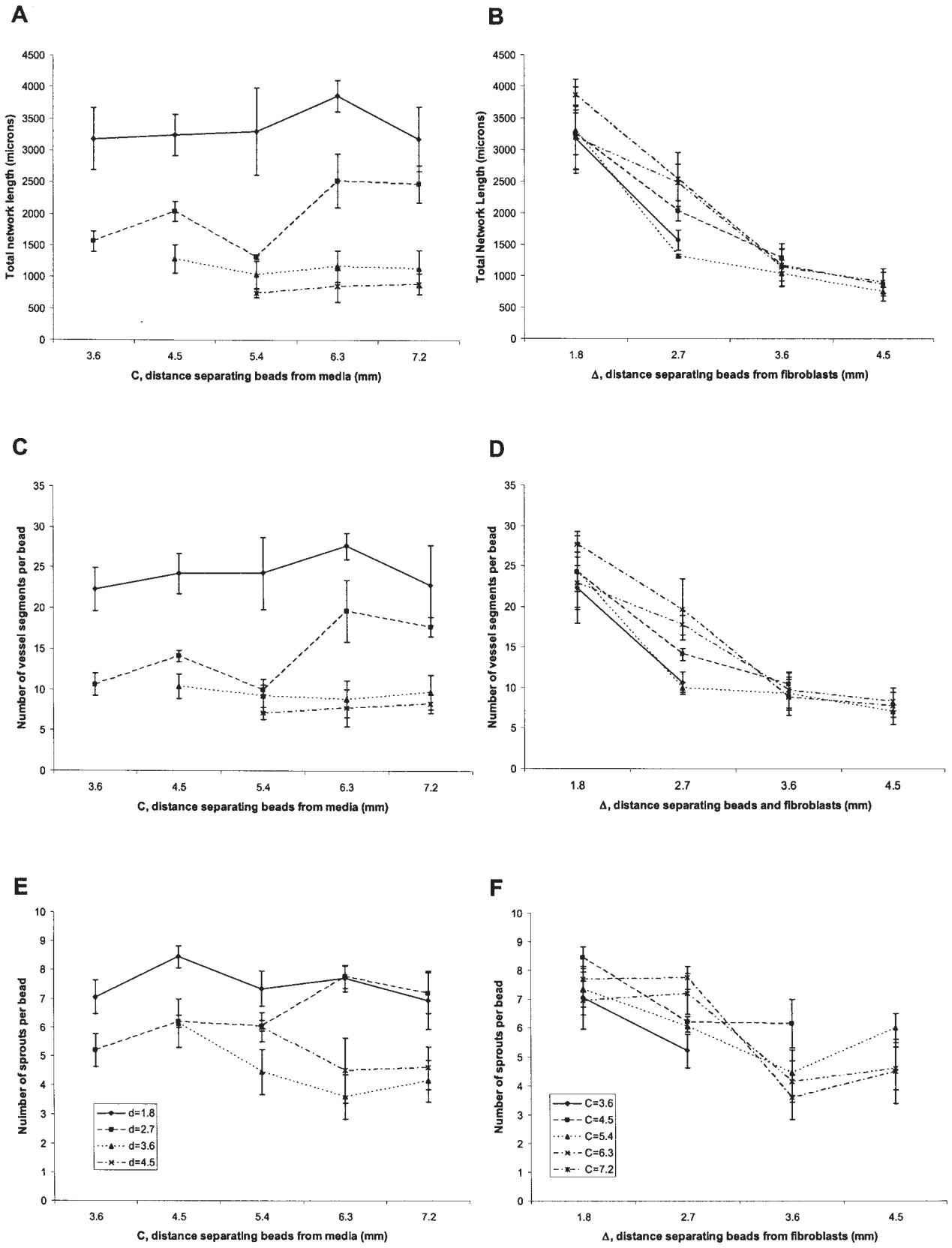
A
Total network length (microns)
C, distance separating beads from media (mm)
B
Total Network Length (microns)
Δ, distance separating beads from fibroblasts (mm)
C
Number of vessel segments per bead
C, distance separating beads from media (mm)
D
Number of vessel segments per bead
Δ, distance separating beads and fibroblasts (mm)
E
Nuimber of sprouts per bead
d=1.8
d=2.7
d=3.6
d=4.5
C, distance separating beads from media (mm)
F
Number of sprouts per bead
C=3.6
C=4.5
C=5.4
C=6.3
C=7.2
Δ, distance separating beads from fibroblasts (mm)

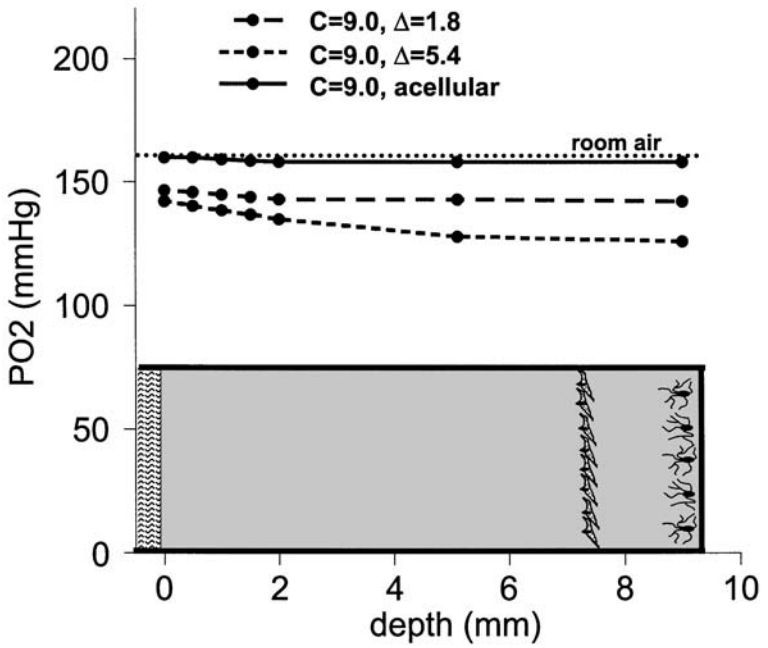

FIG. 6. Oxygen tension *in vitro* is nearly constant throughout the depth of a 9-mm tissue construct. Oxygen tension as a function of depth into the fibrin-based construct is reported in both an acellular gel and two standard gels with fibroblasts and a capillary network. The capillary network is 9.0 mm from the nutrient medium (i.e., $C = 9.0$ mm) with values of Δ equally 1.8 and 5.4 mm, respectively. The data points are means of measurements from three different positions at each depth in a single construct. Standard error of these measurements was $<2\%$. The top (depth = 0 mm) of the gel is exposed to room air. The thin dashed line represents the oxygen tension in room air, and the orientation of the construct is shown at the bottom. Note that oxygen tension throughout the gel is nearly constant, independent of the presence of cells, and is >125 mmHg everywhere.

of nutrients and waste products. The first approach includes degradable microcarriers and cellular transfection. Degradable microcarriers can be used to release angiogenic growth factors such as VEGF or basic fibroblast growth factor (bFGF).[11–17] Alternatively, a mammalian cell can be transfected to overexpress an angiogenic cofactor.[26–28] The primary drawback of this approach for the design of thick tissues is the time needed for ingrowth of new vessels from the host. During this time, cells at the interior of the tissue implant are at risk of necrosis because they have no means of support while new vessels penetrate from the edges. Rapid vascularization throughout the entire tissue is needed to overcome this drawback.

The second approach involves the use of degradable polymer scaffolds that can provide bulk and porosity for an implantable device and also encourage the ingrowth of vessels *in vivo*. An early study utilized a degradable poly(glycolic acid) (PGA) scaffold seeded with chondrocytes and demonstrated tissue differentiation, but was limited to a thickness of 0.35 cm.[18] More recently, a macroporous hydrogel bead using sodium alginate covalently coupled with an arginine, glycine, and aspartic acid-containing peptide was demonstrated to maintain bulk and induce the ingrowth of vessels 6 months postimplant in mice.[19] The size of these implantable beads ranged from 2.7 to 3.2 mm in diameter. If the implantable scaffold contains cells of a specific phenotype (i.e., hepatocytes or cardiac myocytes), the primary disadvantage is the reliance on diffusion to deliver nutrients and oxygen while waiting for the ingrowth of new vessels from the host, similar to the first approach. If the scaffold is acellular, then the primary disadvantage is the limitation of the final tissue to fibrovascular scar tissue.

The third approach involves prevascularizing a tissue construct before implantation. One strategy is to prevascularize a tissue by implanting a degradable polymeric construct into a host, allowing a fibrovascular tissue to develop. Then, inject cells specific to the tissue function of interest (e.g., hepatocytes).[20] This strategy is again limited by the need for ingrowth of new vessels into the initial polymer construct.

In vitro *diffusion barriers*

The current study advances our understanding of diffusion barriers *in vitro* by examining two critical distances that separate the developing capillary network from necessary growth factors and nutrients. It is clear that the fibroblast produces soluble mediators (i.e.,

growth factors) that diffuse through the fibrin matrix to the HUVECs. In the absence of the fibroblast, mature capillaries are not produced, and as the fibroblast monolayer is moved to distances greater than approximately 1.8 mm, the extent of the capillary network in terms of length and number of vessel sprouts is significantly compromised. Although the specific factors produced by the fibroblast are as yet not identified, potential candidates included bFGF, platelet-derived growth factor (PDGF),[26] transforming growth factor β (TGF-β),[29] and the angiopoietins (Ang),[30] which are all known to participate in the stimulation and stabilization of new capillaries.

Our data also suggest that the factors produced by the fibroblast are more sensitive to diffusion distance than those present in the growth medium. The quality of the capillary network was compromised when the fibroblast monolayer was moved more than 1.8 mm from the HUVEC-coated beads; however, the capillary network was not compromised by moving the growth medium to distances as great as 7.2 mm away from the capillary network. Finally, diffusion of oxygen does not appear to be limiting *in vitro*. For gel thickness less than 9 mm, our lowest measurements of oxygen tension still exceeded 125 mmHg; typical partial pressures of oxygen in tissue are as low as 25 mmHg. This important finding allows the development of vascular networks *in vitro* in tissue constructs on the order of centimeters in thickness, which is critical as the vascular network is not yet functional (i.e., delivering oxygen and removing carbon dioxide). Once implanted, rapid integration with the host vascular system is anticipated on the basis of observations *in vivo*, which have shown the dynamic development of mature vascular systems in less than 24 h.[31] Thus, it is anticipated that increased oxygen demands from invading host cells will be met by the preformed, but now functional, vascular network.

The lack of an observable diffusion limitation for oxygen in our *in vitro* model is likely to due to physical properties of the matrix, such as fibrin concentration or cell density, which differ from the *in vivo* environment. Although mimicking *in vivo* oxygen diffusion was not the goal of the current experiment, future investigation may simulate these conditions by increasing cell density, distributing DFs throughout the fibrin matrix, or altering the concentration of fibrin. These perturbations may allow a more specific examination of oxygen transport on capillary formation.

Conclusion

In summary, we have established a model of angiogenesis using human umbilical vein endothelial cells, dermal fibroblasts, and a fibrin matrix. The construct demonstrates robust capillary growth with clear lumens that reach lengths greater than 500 μm by 6 days in culture, and complex anastomosing capillary networks after 14 days in culture. Oxygen diffusion is not limiting *in vitro*, allowing the creation of prevascularized tissue constructs on the order of centimeters in thickness. Soluble factors produced from the fibroblasts are necessary to stabilize the capillary network, and are more sensitive to diffusion distance than soluble factors in the growth medium. This model of angiogenesis mimicks the architecture of a healing wound, and may provide a framework for the design of thicker engineered tissues beyond the diffusion limit ($>$2 mm) that currently limits the field of tissue engineering.

ACKNOWLEDGMENTS

This project was supported in part by seed grants from the the Council on Research, Computing, and Library Resources (CORCLR) and the Department of Biomedical Engineering at the University of California, Irvine, as well as the National Institutes of Health (HL60067 and AI40710). We thank Mr. Adrian Fernandez, Mr. Brandon Lee, and Mr. Elbert Jacinto for assistance in quantifying the capillary network. In addition, we also thank Dr. Robert L. Newcomb, Director of the Center for Statistical Consulting at UCI, for assistance in the statistical analysis of the data.

REFERENCES

1. Obradovic, B., Carrier, R.L., Vunjak-Novakovic, G., and Freed, L.E. Gas exchange is essential for bioreactor cultivation of tissue engineered cartilage. Biotechnol. Bioeng. **63,** 197, 1999.
2. Bryant, S.J., and Anseth, K.S. The effects of scaffold thickness on tissue engineered cartilage in photocrosslinked poly(ethylene oxide) hydrogels. Biomaterials **22,** 619, 2001.
3. Martin, I., Vunjak-Novakovic, G., Yang, J., Langer, R., and Freed, L.E. Mammalian chondrocytes expanded in the presence of fibroblast growth factor 2 maintain the ability to differentiate and regenerate three-dimensional cartilaginous tissue. Exp. Cell Res. **253,** 681, 1999.
4. Li, R.K., Yau, T.M., Weisel, R.D., Mickle, D.A., Sakai, T., Choi, A., and Jia, Z.Q. Construction of a bioengineered cardiac graft. J. Thorac. Cardiovasc. Surg. **119,** 368, 2000.
5. Bursac, N., Papadaki, M., Cohen, R.J., Schoen, F.J., Eisenberg, S.R., Carrier, R., Vunjak-Novakovic, G., and Freed, L.E. Cardiac muscle tissue engineering: Toward an *in vitro* model for electrophysiological studies. Am. J. Physiol. **277,** H433, 1999.
6. Papadaki, M., Bursac, N., Langer, R., Merok, J., Vunjak-Novakovic, G., and Freed, L.E. Tissue engineering of functional cardiac muscle: Molecular, structural, and electrophysiological studies. Am. J. Physiol. Heart Circ. Physiol. **280,** H168, 2001.

7. Patrick, C.W., Jr., Chauvin, P.B., Hobley, J., and Reece, G.P. Preadipocyte seeded PLGA scaffolds for adipose tissue engineering. Tissue Eng. **5,** 139, 1999.
8. Kim, B.S., Putnam, A.J., Kulik, T.J., and Mooney, D.J. Optimizing seeding and culture methods to engineer smooth muscle tissue on biodegradable polymer matrices. Biotechnol. Bioeng. **57,** 46, 1998.
9. Zandonella, C. The beat goes on. Nature **421,** 884, 2003.
10. American Society of Plastic Surgery. 2000 Reconstructive Surgery Trends. See http://www.plasticsurgery.org/public_education/2000statistics.cfm
11. Tabata, Y., Miyao, M., Ozeki, M., and Ikada, Y. Controlled release of vascular endothelial growth factor by use of collagen hydrogels. J. Biomater. Sci. Polym. Ed. **11,** 915, 2000.
12. Peters, M.C., Polverini, P.J., and Mooney, D.J. Engineering vascular networks in porous polymer matrices. J. Biomed. Mater. Res. **60,** 668, 2002.
13. Lee, K.Y., Peters, M.C., Anderson, K.W., and Mooney, D.J. Controlled growth factor release from synthetic extracellular matrices. Nature **408,** 998, 2000.
14. Hopkins, S.P., Bulgrin, J.P., Sims, R.L., Bowman, B., Donovan, D.L., and Schmidt, S.P. Controlled delivery of vascular endothelial growth factor promotes neovascularization and maintains limb function in a rabbit model of ischemia. J. Vasc. Surg. **27,** 886, (discussion, p. 895), 1998.
15. Elcin, Y.M., Dixit, V., and Gitnick, G. Extensive *in vivo* angiogenesis following controlled release of human vascular endothelial cell growth factor: Implications for tissue engineering and wound healing. Artif. Organs **25,** 558, 2001.
16. Cleland, J.L., Duenas, E.T., Park, A., Daugherty, A., Kahn, J., Kowalski, J., and Cuthbertson, A. Development of poly-(D,L-lactide—coglycolide) microsphere formulations containing recombinant human vascular endothelial growth factor to promote local angiogenesis. J. Control. Release **72,** 13, 2001.
17. King, T.W., and Patrick, C.W., Jr. Development and *in vitro* characterization of vascular endothelial growth factor (VEGF)-loaded poly(DL-lactic-co-glycolic acid)/poly(ethylene glycol) microspheres using a solid encapsulation/single emulsion/solvent extraction technique. J. Biomed. Mater. Res. **51,** 383, 2000.
18. Freed, L.E., Vunjak-Novakovic, G., Biron, R.J., Eagles, D.B., Lesnoy, D.C., Barlow, S.K., and Langer, R. Biodegradable polymer scaffolds for tissue engineering. Biotechnology **12,** 689, 1994.
19. Loebsack, A., Greene, K., Wyatt, S., Culberson, C., Austin, C., Beiler, R., Roland, W., Eiselt, P., Rowley, J., Burg, K., Mooney, D., Holder, W., and Halberstadt, C. *In vivo* characterization of a porous hydrogel material for use as a tissue bulking agent. J. Biomed. Mater. Res. **57,** 575, 2001.
20. Fontaine, M., Schloo, B., Jenkins, R., Uyama, S., Hansen, L., and Vacanti, J.P. Human hepatocyte isolation and transplantation into an athymic rat, using prevascularized cell polymer constructs. J. Pediatr. Surg. **30,** 56, 1995.
21. Frerich, B., Lindemann, N., Kurtz-Hoffmann, J., and Oertel, K. *In vitro* model of a vascular stroma for the engineering of vascularized tissues. Int. J. Oral Maxillofac. Surg. **30,** 414, 2001.
22. Schechner, J.S., Nath, A.K., Zheng, L., Kluger, M.S., Hughes, C.C., Sierra-Honigmann, M.R., Lorber, M.I., Tellides, G., Kashgarian, M., Bothwell, A.L., and Pober, J.S. *In vivo* formation of complex microvessels lined by human endothelial cells in an immunodeficient mouse. Proc. Natl. Acad. Sci. U.S.A. **97,** 9191, 2000.
23. Ordemann, R., Holig, K., Wagner, K., Rautenberg, U., Bornhauser, M., Kroschinsky, F., Schafer, J., Schuler, U., and Ehninger, G. Acceptance and feasibility of peripheral stem cell mobilisation compared to bone marrow collection from healthy unrelated donors. Bone Marrow Transplant. **21**(Suppl. 3)**,** S25, 1998.
24. Demirer, T., Buckner, C.D., and Bensinger, W.I. Optimization of peripheral blood stem cell mobilization. Stem Cells **14,** 106, 1996.
25. Balconi, G., Spagnuolo, R., and Dejana, E. Development of endothelial cell lines from embryonic stem cells: A tool for studying genetically manipulated endothelial cells *in vitro*. Arterioscler. Thromb. Vasc. Biol. **20,** 1443, 2000.
26. Soker, S., Machado, M., and Atala, A. Systems for therapeutic angiogenesis in tissue engineering. World J. Urol. **18,** 10, 2000.
27. Zaric, V., Weltin, D., and Stephan, D. Therapeutic angiogenesis using genetic transfection: An *in vitro* quantitative and functional study after gene code transfer for vascular endothelial growth factor. Arch. Mal. Coeur Vaiss. **93,** 987, 2000.
28. Ajioka, I., Nishio, R., Ikekita, M., Akaike, T., Sasaki, M., Enami, J., and Watanabe, Y. Establishment of heterotropic liver tissue mass with direct link to the host liver following implantation of hepatocytes transfected with vascular endothelial growth factor gene in mice. Tissue Eng. **7,** 335, 2001.
29. Pepper, M.S. Transforming growth factor-β: Vasculogenesis, angiogenesis, and vessel wall integrity. Cytokine Growth Factor Rev. **8,** 21, 1997.
30. Hanahan, D. Signaling vascular morphogenesis and maintenance. Science **277,** 48, 1997.
31. Lawson, N.D., and Weinstein, B.M. *In vivo* imaging of embryonic vascular development using transgenic zebrafish. Dev. Biol. **248,** 307, 2002.

Address reprint requests to:
Steven C. George, M.D., Ph.D.
Department of Biomedical Engineering
204 Rockwell Engineering Center
University of California, Irvine
Irvine, CA 92697-2715

E-mail: scgeorge@uci.edu